20

Theory and Physiology of Electrical Stimulation of the Central Nervous System

Warren M. Grill

20.1 Introduction

Electrical stimulation is a widespread method to study the form and function of the nervous system and a technique to restore function following disease or injury. The central nervous system (CNS) includes the brain and spinal cord (Figure 20.1). Both the spinal cord and brain include regions primarily populated by cell bodies (somas) of neurons, and termed gray matter for its color, and regions primarily populated by axons of neurons, and termed white matter. The diversity of neuronal elements and the complexity of the volume conductor make understanding the effects of stimulation more challenging in the case of CNS stimulation than in the case of peripheral stimulation. Specifically, it is unclear, in many cases, what neuronal elements (axons, cell bodies, pre-synaptic terminals; Figure 20.1) are activated by stimulation [Ranck, 1975]. Further, it is unclear how targeted neural elements can be stimulated selectively without co-activation of other surrounding elements. This chapter presents a review of the properties of CNS stimulation as required for rational design and interpretation of therapies employing electrical stimulation.

Electrical stimulation has been used to determine the structure of axonal branching [Jankowska and Roberts, 1972], examine the strength of connections between neurons, and determine the projection

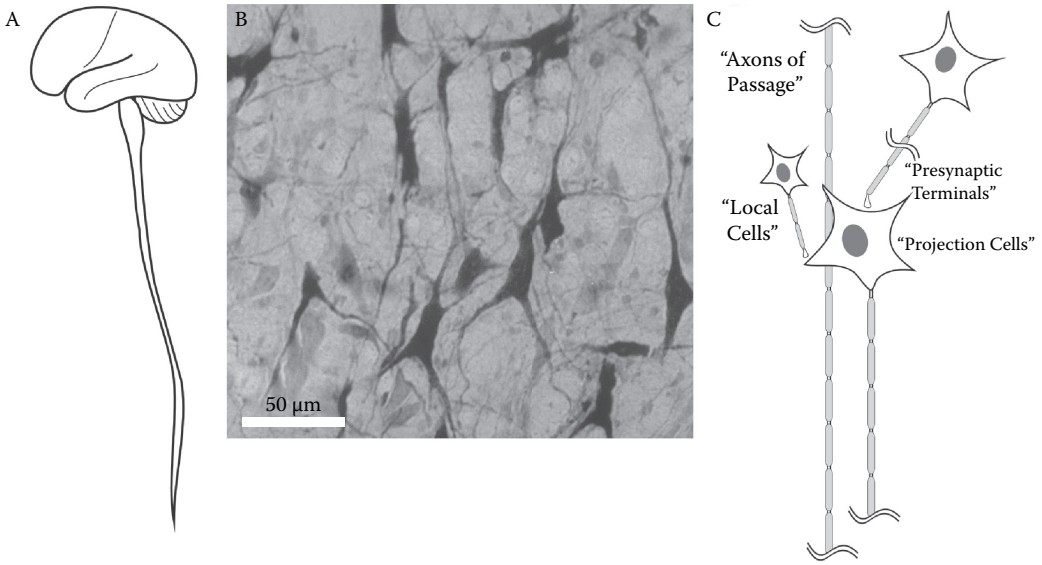

FIGURE 20.1 Structure of the central nervous system. (A) The central nervous system (CNS) includes the brain and spinal cord. (B) The gray matter of the CNS contains the cell bodies of neurons as well as dendritic and axonal processes. (C) When an electrode is placed within the heterogeneous cellular environment of the CNS, it is unclear which neuronal elements are effected by stimulation.

patterns of neurons [Lipski, 1981; Tehovnik, 1996]. Examples of the application of CNS stimulation in treatment of neurological disorders include the treatment of pain by stimulation of the brain [Coffey, 2001] and spinal cord [Cameron, 2004], treatment of tremor and the motor system symptoms of Parkinson's disease [Gross and Lozano, 2000], as an experimental treatment for epilepsy [Velasco et al., 2001; Hodaie et al., 2002], as well as a host of other neurological disorders [Gross, 2004]. In addition, CNS stimulation is being developed for restoration of hearing by electrical stimulation of the cochlear nucleus [Otto et al., 2002] and for restoration of vision [Brindley and Lewin, 1968; Schmidt et al., 1996; Troyk et al., 2003].

A nerve cell or a nerve fiber can be artificially stimulated by depolarization of the cell's membrane. The resulting action potential propagates to the terminal of the neuron, leading to release of neurotransmitters that can impact the post-synaptic cell. Passage of current through extracellular electrodes positioned near neurons creates extracellular potentials in the tissue. The resulting potential distribution can result in an outward-flowing transmembrane current and depolarization. Alternately, extracellular potentials may modulate or block ongoing neuronal firing, depending on the magnitude, distribution, and polarity of the potentials.

The objective of this chapter is to present the biophysical basis for electrical stimulation of neurons in the CNS. The focus is on using a fundamental understanding of both the electric field and its effects on neurons to determine the site of neuronal excitation or modulation in the CNS where electrodes are placed among heterogeneous populations of neuronal elements, including cells, axons, and dendrites.

20.2 Generation of Potentials in CNS Tissues

Passage of current through tissue generates potentials in the tissue (recall Ohm's law: V = IR). The potentials depend on the electrode geometry, the stimulus parameters (current magnitude), and the electrical properties of the tissue. For example, the potential generated by a monopolar point source can be determined analytically using the relationship $V_e(r) = \frac{I}{4\pi\sigma r}$, where I is the stimulating current, σ is the conductivity of the tissue medium (Table 20.1), and r is the distance between the electrode and the

TABLE 20.1 Electrical Conductivity of CNS Tissues

Tissue Type	Electrical Conductivity (S/m)	Ref.
Dura	0.030	Holsheimer et al., 1995
Cerebrospinal fluid	1.5; 1.8	Crile et al., 1922; Baumann et al., 1997
Gray matter	0.20	Ranck, 1963; Li et al., 1968; Sances and Larson, 1975
White matter		Anisotropic
Transverse		
	0.6	Ranck and BeMent, 1965 (cat dorsal columns)
	1.1	Nicholson, 1965 (cat internal capsule)
Longitudinal		
	0.083	Ranck and BeMent, 1965
	0.13	Nicholson, 1965
Encapsulation tissue	0.16	Grill and Mortimer, 1994

AU: Correct placement?

measurement point. The point source model is a valid approximation for sharp electrodes with small tips [McIntyre and Grill, 2001]. Larger electrodes are typically used for chronic stimulation of the CNS, and the spatial distribution of the potentials in the tissue differs from those produced by a point source electrode (Figure 20.2). Examples of the spectrum of electrode types used for CNS stimulation (and recording) are shown in Figure 20.3.

The extracellular potentials generated by the passage depend on the electrical properties of the tissue. The electrical properties of peripheral nerves are both inhomogeneous and anisotropic (Table 20.1), and the distribution of potentials within the nerve will depend strongly on the nerve and electrode geometries. In general, biological conductivities have a small reactive component [Ackman and Seitz, 1984; Eisenberg and Mathias, 1980], and thus a relatively small increase in conductivity at higher frequencies [Ranck, 1963; Nicholson, 1965; Ranck and BeMent, 1965].

Spatial variations in the electrical properties of the tissue can cause changes in the patterns of activation (Grill, 1999). In most cases, to calculate accurately the extracellular potentials generated by extracellular stimulation requires a numerical solution using a discretized model, for example with the finite element method (e.g., Veltink et al., 1989; McIntyre and Grill, 2002).

20.3 Response of Neurons to Imposed Extracellular Potentials

As described in the previous section, the distribution of extracellular potentials depends on the electrode geometry, the electrical properties of the extracellular tissue, and the stimulation amplitude. The effect of the potentials on neurons depends on the nerve cell type, its size and geometry, as well as the temporal characteristics of the stimulus. During stimulation of peripheral nerves, it is clear that it is the axons in the vicinity of the electrodes that are activated. However, the CNS contains a heterogeneous population of neuronal elements, including local cells projecting locally around the electrode, as well as those projecting away from the region of stimulation, axons passing by the electrode, and pre-synaptic terminals projecting onto neurons in the region of the electrode (Figure 20.1C). The effects of stimulation can be mediated by activation of any or all of these elements and include both the direct effects of stimulation of post-synaptic elements, as well as the indirect effects mediated by electrical stimulation of pre-synaptic terminals that mediate the effects of stimulation via synaptic transmission.

From this complexity arise two principal questions during stimulation of the CNS [Grill and McIntyre, 2001]: (1) what neuronal elements are activated by extracellular stimulation?, and (2) how can targeted elements be stimulated selectively? Computational modeling provides a powerful tool to study extracellular excitation of CNS neurons. The volume of tissue stimulated, both for fibers and cells, and how this changes with electrode geometry, stimulus parameters, and the geometry of the neuronal elements are quite challenging to determine experimentally. Using a computer model enables examination of these parameters under controlled conditions, and enables simultaneous determination of the effects of stimulation on all the different neural elements around the electrode. Computational modeling of the effects

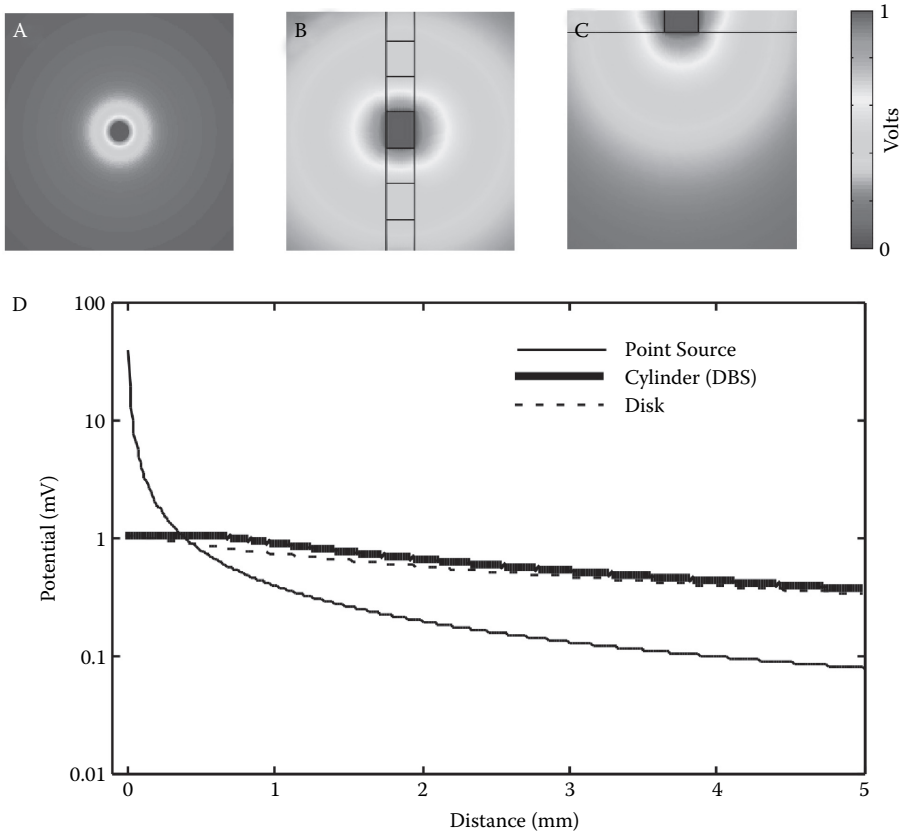

FIGURE 20.2 Electric fields generated by the passage of current in CNS tissue. The first step in determining the response of CNS neurons to extracellular stimulation is to calculate the electric potentials generated in the tissue by passing current through the electrode. Potentials produced by passing current into a homogenous region of the CNS (s = 0.2 S/m) using a point-source electrode (A), a cylindrical electrode (B) as used for deep brain stimulation, and a disk electrode (C) as used for epidural or cortical surface stimulation. (D) Although a simple analytical solution exists for the potentials generated by a point-source electrode, they differ substantially from the potentials generated by larger cylindrical or disk electrodes.

of extracellular stimulation on neurons involves a two-step approach. The first step is to calculate the electric potentials generated in the tissue by passage of current through the electrode. The second step is to determine the effect (or effects) of those potentials on the surrounding neurons.

20.4 From Cell to Circuit: Construction of Models of CNS Neurons

Electrical circuits are used to model the electrical behavior of neurons. These electrical-equivalent circuits, often referred to as cable models, represent the neuron as a series of cylindrical elements. Each cylinder is, in turn, replaced by a "compartment," representing the neuronal membrane, and a resistor representing the intracellular space. Thus, the model becomes a series of membrane compartments, connected by resistors. Each compartment is itself an electrical circuit that includes a capacitor representing the membrane capacitance of the lipid bilayer, resistors representing the ionic conductances of the transmembrane proteins (ion channels), and batteries representing the differences in potential (Nernst potential) arising from ionic concentration differences across the membrane. The process of constructing an equivalent electric circuit model of a CNS neuron is illustrated in Figure 20.4.

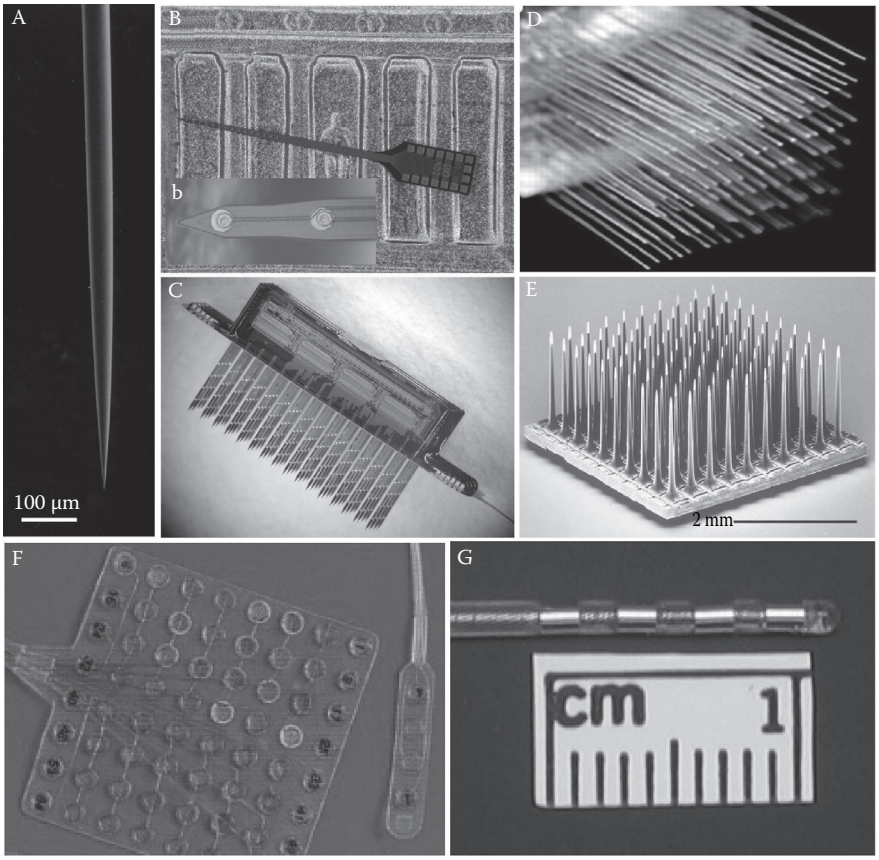

FIGURE 20.3 Electrodes for central nervous system stimulation. (A) Single iridium microwire electrode developed at Huntington Medical Research Institutes that can be used for extracellular recording from single units or extracellular microstimulation of small populations of neurons [McCreery et al., 1997] (B) Multisite silicon microprobe developed at the University of Michigan and higher magnification view (b) of two electrode sites near the tip. (Images courtesy of J.F. Hetke, University of Michigan.) (C) Three-dimensional assembly of multisite silicon microprobes [Bai et al., 2000]. The array is four probes, 256 sites on 400-µm centers in three dimensions. There are 16 parallel stimulating channels (16 sites active at any time) with off-chip current generation. The array is fed by a 7-lead ribbon cable at a data rate of up to 10 Mbps. It operates from ±5V supplies. (Image courtesy of K.D. Wise, University of Michigan.) (D) Arrays of up to 128 microwires enable simultaneous extracellular recording from multiple single neurons. Each wire is 50-µm diameter stainless steel, insulated with Teflon [Nicolelis et al., 2003]. (E) Multi-electrode silicone array developed at the University of Utah [Normann et al., 1999]. (F) Subdural grid and strip electrode arrays used for cortical stimulation and recording (PMT Corporation, Chanhassen, Minnesota). (G) Quadrapolar electrode used for deep brain stimulation (Medtronic Inc., Minneapolis, Minnesota).

One can readily calculate the values of circuit elements from the geometry of the neurons and the specific values of neuron electrical properties. Consider a cylindrical representation of a segment of neuronal element, with diameter d and length l (Figure 20.4E). If one cuts and "unrolls" the cylinder, then the membrane resistance, R_m, is calculated as:

$$R_m = \text{Specific membrane resistance} / \text{Area of segment}$$

$$= r_m / \pi * l * d$$

AU: correct value

where typical values for the specific membrane resistance range from 1000 to 5000 400 Ω-cm^2. The membrane resistance is nonlinear, its value depending on the voltage across the membrane (transmembrane

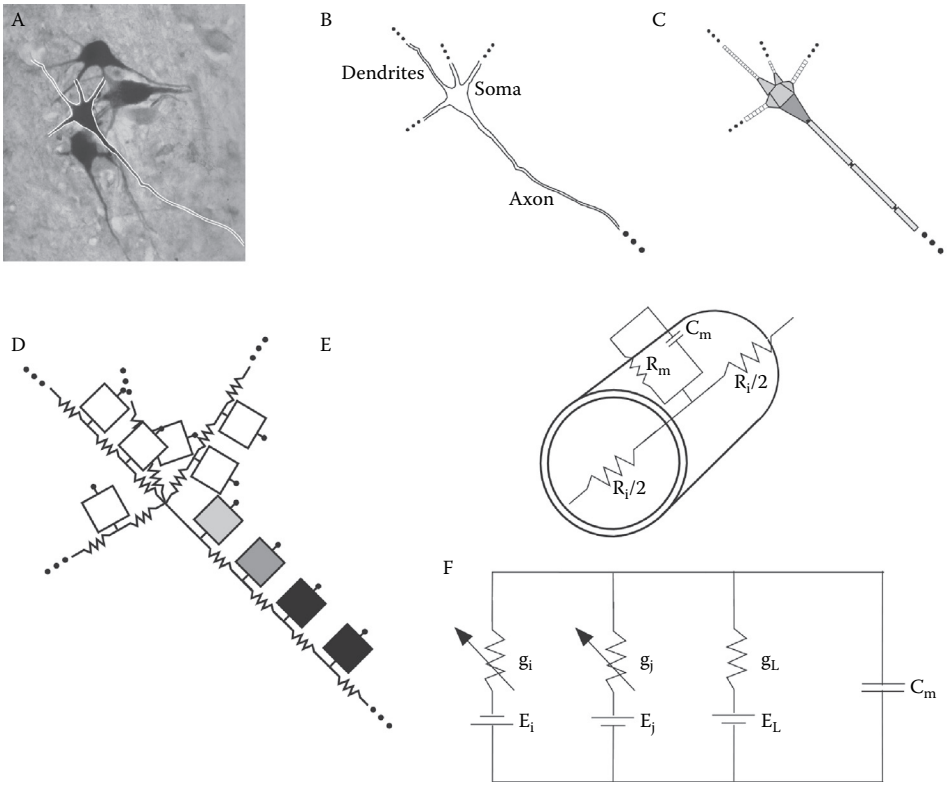

FIGURE 20.4 Construction of models of central nervous system (CNS) neurons. (A) Examples of stained neurons in the CNS. (B) The morphology of stained neurons can be reconstructed in three dimensions. (C) The morphology is then converted into a series of equivalent cylindrical elements. (D) The cylindrical elements are subsequently replaced by electrical equivalent circuits with resistive elements representing the intracellular space, and compartmental models representing the membrane. (E) Each cylindrical segment includes a representation of the membrane and the intracellular space, and the values of the equivalent circuit elements can be calculated from the geometry of the cylinder and specific parameter values. (F) Each compartment model of the membrane may contain several nonlinear ionic conductances (g_i, g_j) and a linear ionic conductance (g_L) representing various ionic channels in the membrane, batteries representing the Nernst potential arising from the difference in concentration of ions on the inside and outside of the membrane (E_i, E_j, E_L), and a capacitor (C_m) representing the capacitance arising from the lipid bilayer of the cell.

potential). Further, separate elements (typically calculated as conductances) are used to represent the transmembrane paths for different ionic species, and the model of a patch of membrane includes several of these in parallel (Figure 20.4E). Similarly, the membrane capacitance, C_m, can be calculated as:

$$C_m = \text{Specific membrane capacitance} * \text{Area of segment}$$

$$= c_m / \pi * l * d$$

where typical values of the specific membrane capacitance range between 1 and 2 μF/ cm^2. The intracellular resistance, R_i, can be calculated as:

$$R_i = \text{Intracellular resistivity} * \text{Segment length} / \text{Cross-sectional area of segment}$$

$$= \rho_i * l / (\pi*(d/2)^2)$$

where typical values of the intracellular resistivity range from 50 to 400 Ω-cm.

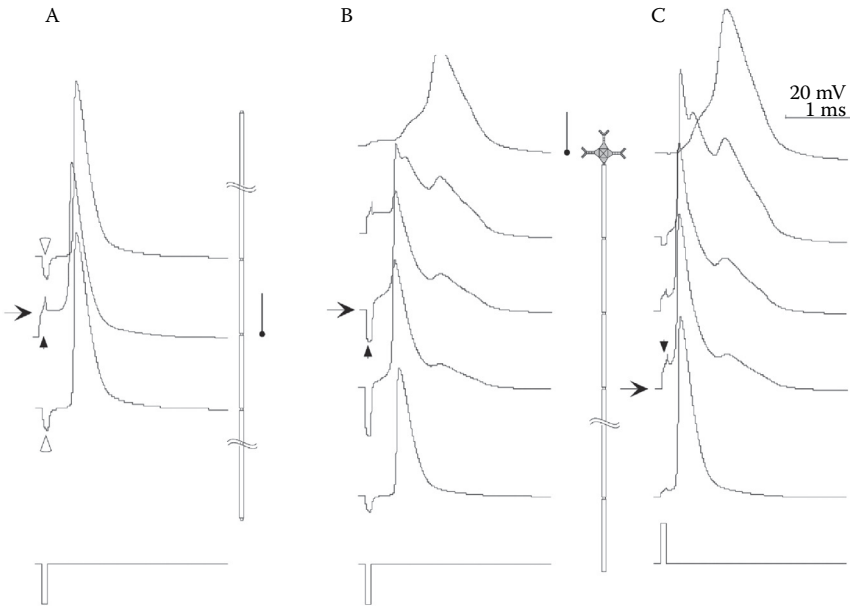

FIGURE 20.5 Action potential initiation by extracellular stimulation in CNS neurons by cathodic and anodic stimuli. Each trace shows transmembrane voltage as a function of time for different sections of the neuron. (A) Stimulation with a monophasic cathodic stimulus pulse from an electrode positioned 1 mm over a node of Ranvier of the axon. Depolarization occurs in the node directly beneath the electrode (solid arrowhead), and hyperpolarization occurs in the adjacent nodes of Ranvier (open arrowhead). Action potential initiation occurs in the node of Ranvier directly under the electrode (arrow), and the action potential propagates in both directions. (B) During threshold stimulation with an electrode positioned 1 mm over the cell body, action potential initiation occurs at a node of Ranvier of the axon. With cathodic stimuli (duration 0.1 ms), action potential initiation occurred at the second node of Ranvier from the cell body (arrow). (C) With anodic stimuli (duration 0.1 ms), action potential initiation occurred in the third node of Ranvier from the cell body (arrow).

20.5 Sites of Action Potential Initiation in CNS Neurons

The response of a cable model, representing a CNS neuron, to extracellular electrical stimulation is shown in Figure 20.5. The transmembrane potential as a function of time, in different segments of the neuron, is shown for a cathodic electrode positioned over the axon (Figure 20.5A), for a cathodic electrode positioned over the cell body (Figure 20.5B), and for an anodic electrode positioned over the cell body (Figure 20.5C).

During stimulation over the axon with a cathodic current, the axon is depolarized immediately beneath the electrode and hyperpolarized in regions lateral to the electrode (arrowheads in Figure 20.5A). Action potential initiation occurs in the most depolarized node of Ranvier, immediately beneath the electrode (arrow) and then propagates in both directions.

The response of a CNS neuron is more complex. With both cathodic and anodic stimuli delivered through an electrode placed 1 mm above the cell body, action potential initiation occurred in the axon, although the electrode is positioned directly over the soma. With 0.1-ms duration cathodic stimuli, action potential initiation occurred at the second node of Ranvier from the cell body (arrow); and with 0.1-ms duration anodic stimuli, action potential initiation occurred in the third node of Ranvier from the cell body (arrow). During the cathodic stimulus pulse, the node of Ranvier where action potential initiation occurred was hyperpolarized by the stimulus (arrowhead). Following termination of the stimulus, the cell body and dendritic tree discharged through the axon, leading to action potential initiation [McIntyre and Grill, 1999]. This finding in a computational model is consistent with contemporary *in vitro* results from cortex [Nowak and Bullier, 1998a,b]. Thus, with cathodic stimuli, action potential initiation

occurred in a part of the neuron that was hyperpolarized by the stimulus, and this indirect mode of activation increases the threshold for activation of local cells with cathodic stimuli. Conversely, with anodic stimuli, the site of action potential initiation was at the node that was most depolarized by the stimulus (arrowhead). These position-dependent thresholds also are reflected in exciting populations of neurons (see below).

20.6 Excitation Properties of CNS Stimulation

The finding that action potential initiation occurs in the axon has several important implications for CNS stimulation. First, because excitation occurs in the axon, there is little difference in the extracellular chronaxie times for excitation of local cells and excitation of passing axons (see "Strength-Duration Relationship" below). Therefore, chronaxie time is not a sensitive indicator of the neuronal element that is activated by extracellular stimulation [Miocinovic and Grill, 2004]. Second, because action potential initiation occurs at some distance from the site of integration of synaptic inputs, the effects of co-activation of pre-synaptic fibers may be less than expected, and the axon may still fire even when the cell body is hyperpolarized (e.g., by inhibitory synaptic inputs) (see "Indirect Effects" below). Therefore, extracellular unit recordings of cell body firing may not accurately reflect the output of the neuron [Grill and McIntyre, 2001; McIntyre et al., 2004]. Finally, the difference in the mode of activation of local cells by cathodic stimuli and anodic stimuli is the basis for the difference in threshold between cathodic and anodic stimuli (see "Effect of Stimulus Polarity" below).

20.6.1 Strength-Duration Relationship

The stimulus amplitude necessary for excitation, I_{th}, increases as the duration of the stimulus decreases. The strength-duration relationship describes this phenomena and is given by:

$$I_{th} = I_{rh}[1 + T_{ch}/PW]$$

where the parameter I_{rh} is the rheobase current and is defined as the current amplitude necessary to excite the neuron with a pulse of infinite duration, and the parameter T_{ch} is the chronaxie and is defined as the pulse duration necessary to excite the neuron with a pulse amplitude equal to twice the rheobase current.

Measurements with intracellular stimulation have demonstrated that the temporal excitation characteristics, including chronaxie (T_{ch}) and refractory period, of cells and axons differ (Figure 20.6A). However, during extracellular stimulation of neurons, action potential initiation occurs in the axon, even with the stimulating electrode positioned over the cell body or dendrites (see above). Although with intracellular activation the chronaxies of many cell bodies exceed 1 ms, with extracellular activation they are below 1 ms [Stoney et al., 1968; Ranck, 1975; Asanuma, 1976; Swadlow, 1992] and lie within the ranges determined for extracellular activation of axons [Ranck, 1975; Li and Bak, 1976; West and Wolstencroft, 1983]. For stimulation of cortical gray matter, the mean T_{ch} for *intracellular* stimulation of cells (15 ms) was substantially longer than T_{ch} for *extracellular* stimulation of axons (0.27 ms), the mean T_{ch} for *extracellular* stimulation of local cells (0.38 ms) was comparable to that for extracellular stimulation of axons [Nowak and Bullier, 1998a]. Further, during extracellular stimulation, the chronaxies measured with extracellular stimulation depended on a number of factors other than the neuronal element that was stimulated [Miocinovic and Grill, 2004]. The chronaxies of different neuronal elements determined with extracellular stimulation overlap and do not enable unique determination of the neuronal element stimulated.

20.6.2 Current-Distance Relationship

The current required for extracellular stimulation of neurons (threshold, I_{th}) increases as the distance between the electrode and the neuron (r) increases. This is described by the current-distance relationship [Stoney et al., 1968]:

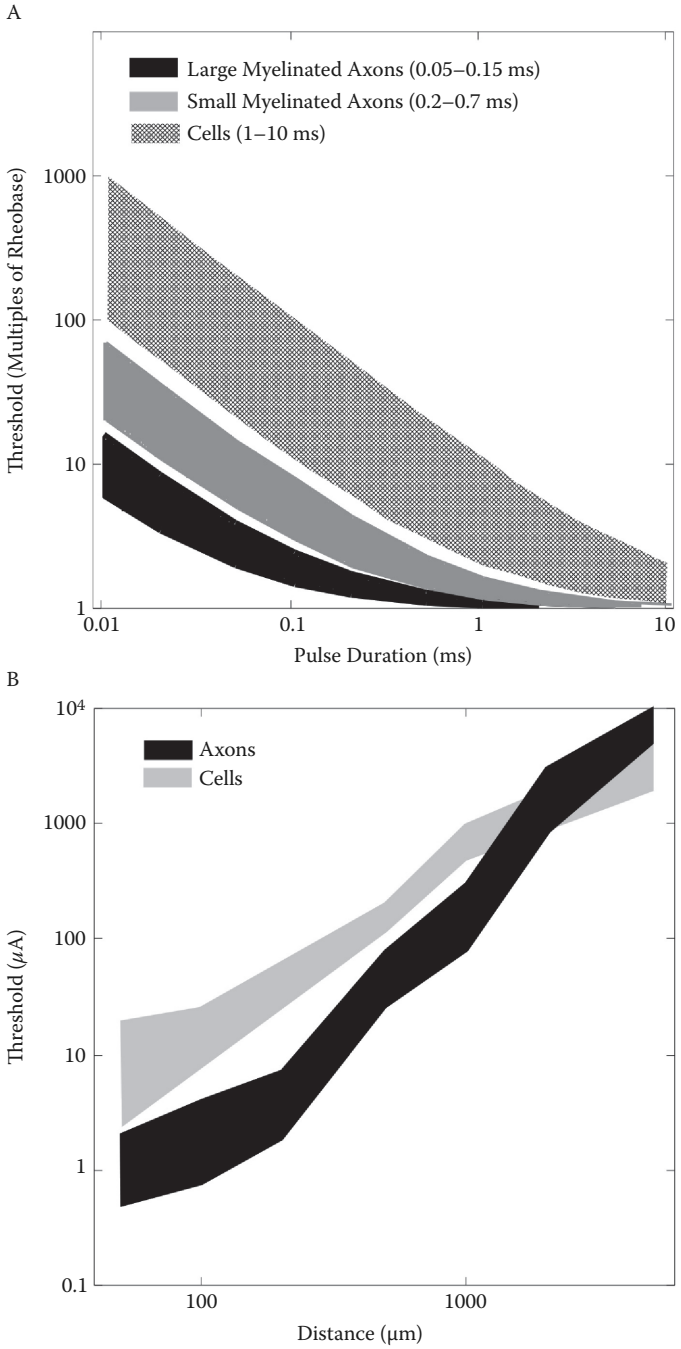

FIGURE 20.6 Properties of central nervous system stimulation. (A) The strength-duration relationship describes the amplitude required for stimulation as a function of the stimulation pulse duration. Strength-duration curves for intracellular stimulation of different neural elements were constructed from data summarized by Ranck (1976). (B) The current-distance relationship describes the threshold intensity required for stimulation as a function of the distance between the electrode and the neuron. Current distance curves for axons and cells were constructed from data summarized by Ranck (1976).

$$I_{th} = I_R + k \cdot r^2$$

where the offset (I_R) determines the absolute threshold and the slope (k) determines the threshold difference between neurons at different distances from the electrode. The current-distance relationship for excitation of axons and cells in the CNS have been measured in a large number of preparations, and current distance curves for these two populations are summarized in Figure 20.6B.

20.6.3 Effect of Stimulus Polarity and Stimulus Waveform on CNS Stimulation

During excitation of axons in the peripheral nervous system, different stimulus polarities produce changes in the threshold as well as changes in the site of action potential initiation, and similar but more pronounced effects occur during CNS stimulation. Figure 20.7 shows the results of a computational study to determine which neuronal elements are activated by extracellular stimulation in the CNS. A model including populations of local cells and axons of passage, randomly positioned around a point source stimulating electrode, was used to compare the activation of local cells to the activation of passing fibers with different stimulation waveforms [McIntyre and Grill, 2000]. Using cathodic pulses, the threshold for activation of passing axons was less than the threshold for activation of local neurons; and when 70% of the axons were activated, approximately 10% of the local cells were also activated. When using anodic pulses, the threshold for activation of local cells is less than the threshold for activation of passing axons, and when the stimulus amplitude that activated 70% of the local cells also activated 25% of the passing axons. The basis for this effect can be understood by comparing action potential initiation in local cells using cathodic and anodic stimuli described above.

To prevent the possible degradation of the stimulating electrode(s) or damage to the tissue, chronic stimulation is conducted with biphasic stimulus pulses [Lilly et al., 1955; Robblee and Rose, 1990]. The response of passing axons and local cells to symmetric biphasic pulses is shown in Figures 20.7C and 20.7D. Using either anodic-phase first or cathodic-phase first pulses, the threshold for activation of passing axons was less than the threshold for activation of local neurons, and the relative selectivity for axons was lower with either pulse than with monophasic cathodic pulses.

These results and previous experimental evidence demonstrates that different neuronal elements have similar thresholds for extracellular stimulation [Roberts and Smith, 1973; Gustafsson and Jankowska, 1976] and illustrates the need for the design of methods that enable selective stimulation. Stimulus waveforms can be designed explicitly to take advantage of the nonlinear conductance properties of neurons and thereby increase the selectivity between activation of different neuronal elements. Biphasic asymmetrical stimulus waveforms capable of selectively activating either local cells or axonal elements consist of a long-duration, low-amplitude pre-pulse followed by a short-duration, high-amplitude stimulation phase. The long-duration pre-pulse phase of the stimulus is designed to create a sub-threshold depolarizing pre-pulse in the non-target neurons and a hyperpolarizing pre-pulse in the target neurons [Grill and Mortimer, 1995; McIntyre and Grill, 2000]. Recall that during cathodic stimulation, the site of excitation in axons is the depolarized node of Ranvier, while the site of excitation in local cells is a node of Ranvier that is hyperpolarized by the stimulus (Figure 20.5). Conversely, with anodic stimuli, the site of excitation in local cells is a depolarized node of Ranvier, and that the most polarized node of passing axons is hyperpolarized by the stimulus. Thus, the same polarity pre-pulse will produce opposite polarization at the sites of excitation in local cells and passing axons. The effect of this subthreshold polarization is to decrease the excitability of the non-target population and increase the excitability of the target population via alterations in the degree of sodium channel inactivation [Grill and Mortimer, 1995]. Therefore, when the stimulating phase of the waveform is applied, neuronal population targeted for stimulation will be activated with greater selectivity [McIntyre and Grill, 2000]. Asymmetrical charge-balanced, biphasic, cathodic phase first stimulus waveforms result in selective activation of local cells, while asymmetrical charge-balanced, biphasic, anodic phase first stimulus waveforms result in selective activation of fibers of passage. Further, charge balancing is achieved as required to reduce the probability

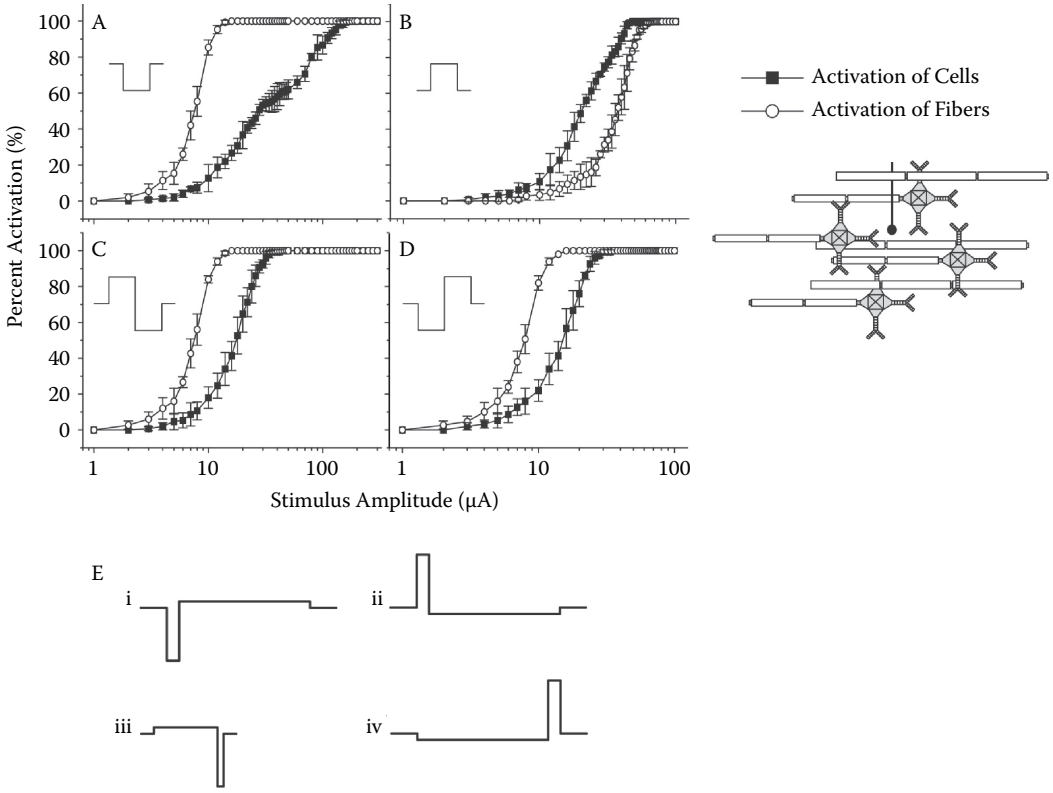

FIGURE 20.7 Effect of stimulus polarity and waveform on excitation of populations of local cells and passing axons. (A to D) Input-output curves from a population model containing 50 passing axons and 50 local cells randomly positioned around a point-source stimulating electrode. The curves are the percent of neurons (passing axons, local cells) activated as a function of the stimulation amplitude for excitation with (A) 0.2-ms duration monophasic cathodic pulses, (B) 0.2-ms duration monophasic anodic pulses, (C) anodic phase first biphasic symmetric pulses (0.2 ms per phase), and (D) cathodic phase first biphasic symmetric pulses (0.2 ms per phase). (Modified from McIntyre and Grill, 2000.) (E) Examples of asymmetric charge-balanced biphasic pulses. Cathodic-phase first (i) and anodic-phase first psuedo-monophasic pulses have low-amplitude second phases and exhibit excitation properties similar to monophasic cathodic and anodic stimuli, respectively. Novel asymmetric pulses that manipulate neuronal excitability via a sub-threshold first that also balances charge that also provides charge balancing. The anodic pre-pulse (0.2 ms) followed by a cathodic stimulus phase (0.02 ms) enables preferential excitation of passing axons, while a cathodic pre-pulse (1.0 ms) followed by an anodic stimulus pulse (0.1 ms) enables preferential excitation of local cells [McIntyre and Grill, 2000].

of tissue damage and electrode corrosion. Note that these pre-pulse waveforms differ from the pseudo-monophasic waveforms used in some stimulators in that the low-amplitude, long-duration phase of the waveform precedes rather than follows the high-amplitude, short-duration phase of the waveform (Figure 20.7E).

20.6.4 Indirect Effects of Extracellular Stimulation

The thresholds for excitation of pre-synpatic terminals and subsequent indirect effects on local neurons (mediated by synaptic transmission) are similar to thresholds for direct effects (mediated by stimulus current) during extracellular stimulation (Figure 20.8A) of spinal cord motoneurons [Gustafson and Jankowska, 1976]; rubrospinal neurons [Baldissera et al., 1972]; and corticospinal neurons [Jankowska et al., 1975]. Further, the chronaxie of pre-synaptic terminals (~0.14 ms in frog spinal cord, Tkacs and Wurster, 1991; 0.06 to 0.54 ms in rat subthalamic nucleus, Hutchison et al., 2002) is comparable to that

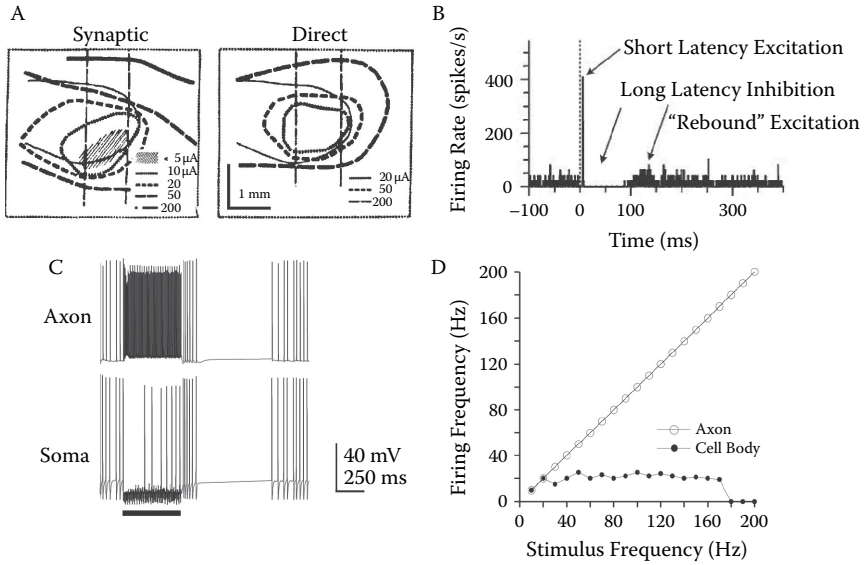

FIGURE 20.8 Central nervous system (CNS) stimulation results in direct effects and indirect effects on CNS neurons. (A) Two-dimensional maps of thresholds for indirect (synaptic) and direct activation of neurons in the red nucleus. (From Baldissera et al., 1972.) (B) Complex poly-phasic changes in the firing rate of a cortical neuron in response to extracellular stimulation. (From Butovas and Schwarz, 2003.) (C) Transmembrane potential in the axon (top trace) and cell body (bottom trace) of a model thalamocortical neuron before, during (black bar at bottom), and after extracellular stimulation. (From McIntyre et al., 2004.) Extracellular stimulation results in simultaneous inhibition of the cell body, as a result of activation of pre-synpatic terminals and subsequent indirect effects, and excitation of the axon, as a result of direct action potential initiation in a node of Ranvier. (D) Firing rate in the cell body and axon during extracellular stimulation of a model thalamocortical neuron (modified from McIntyre et al., 2004). The firing rate in the cell body is lower than that in the axon, as a result of simultaneous indirect synaptic effects on the soma and direct excitation of the axon.

of passing axons, and thus effects may be attributed to activation of passing axons when in fact they arise from activation of pre-synaptic elements. These "indirect" effects of stimulation must be considered when electrodes are placed within the heterogeneous environment of the CNS. During extracellular stimulation, release of inhibitory and/or excitatory neurotransmitters from pre-synaptic terminals can result in complex poly-phasic changes in the firing rate of post-synpatic neurons (Figure 20.8B) [Butovas and Schwarz, 2003] and modulate the threshold for excitation of the post-synaptic neuron [Swadlow, 1992; McIntyre and Grill, 2002]. Thus, indirect effects mediated by synaptic transmission may alter the direct effects of stimulation on the post-synaptic cell. Furthermore, antidromic propagation of action potentials originating from activation of axon terminals can lead to widespread activation or inhibition of targets distant from the site of stimulation through axon collaterals. However, recall that action potential initiation occurs at some distance from the soma, where integration of synaptic inputs occurs, and thus the axon may be excited even when the cell body is hyperpolarized (Figure 20.8C). Therefore, extracellular unit recordings of firing in the soma may not accurately reflect the output of the neuron (Figure 20.8D) [Grill and McIntyre, 2001; McIntyre et al., 2004].

20.7 Summary

This chapter described electrical activation of neurons within the central nervous system (CNS). Electrical stimulation is used to study the form and function of the nervous system and a technique to restore function following disease or injury. Successful application of electrical stimulation to treat nervous

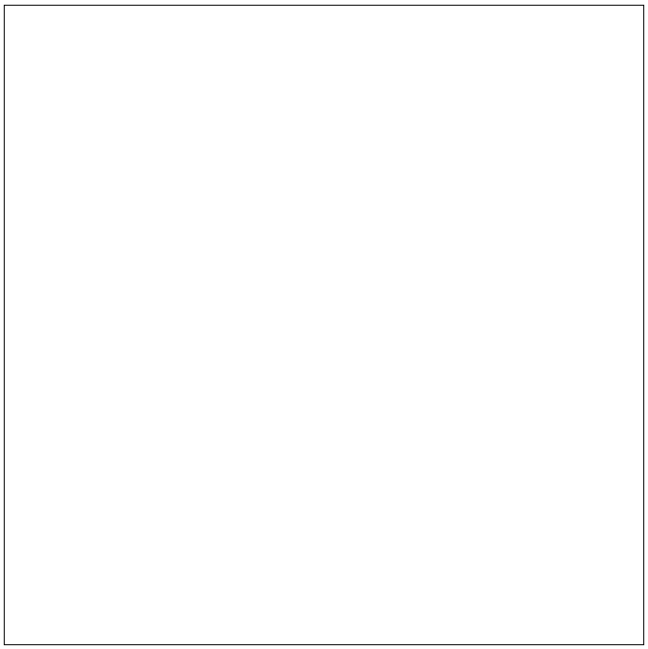

AU: Please provide Figure 20.9

FIGURE 20.9 Charge per phase and charge density are cofactors in determining the threshold for neural damage from CNS stimulation.

system disorders as well as interpretation of the results of stimulation require an understanding of the cellular-level effects of stimulation. Quantitative models provide a means to understand the response of neurons to extracellular stimulation. Further, accurate quantitative models provide powerful design tools that can be used to engineer stimuli that produce a desired response.

The fundamental properties of the excitation of CNS neurons were presented with a focus on what neural elements around the electrode are activated under different conditions. During CNS stimulation, action potentials are initiated in the axons of local cells, even for electrodes positioned over the cell body. The threshold difference between cathodic and anodic stimuli arises due to differences in the mode of activation. Anodic stimuli cause depolarization of the axon and excitation via a "virtual cathode," while cathodic stimuli cause hyperpolarization at the site of excitation and the action potential is initiated during repolarization. The threshold for activation of pre-synaptic terminals projecting into the region of stimulation is often less than or equal to the threshold for direct excitation of local cells, and indirect effects mediated by synaptic transmission may alter the direct effects of stimulation on the post-synaptic cell. The fundamental understanding provided by this analysis enables the rational design and interpretation of studies and devices employing electrical stimulation of the brain or spinal cord.

Acknowledgments

Research in Dr. Grill's laboratory and preparation of this chapter were supported by NIH Grant R01 NS-40894.

References

Ackman, J.J. and Seitz, M.A. (1984). Methods of complex impedancemeasurement in biologic tissue. *CRC Crit. Rev. Biomed. Eng.*, 11:281–311.

Asanuma, H., Arnold, A., and Zarezecki, P. (1976). Further study on the excitation of pyramidal tract cells by intracortical microstimulation. *Exp. Brain Res.*, 26:443–461.

Bai, Q., Wise, K.D., and Anderson, D.J. (2000). A high-yield microassembly structure for three-dimensional microelectrode arrays. *IEEE Trans. Biomed. Eng.,* 47(3):281–9.

Baldissera, F., Lundberg, A., and Udo, M. (1972). Stimulation of pre- and postsynaptic elements in the red nucleus. *Exp. Brain Res.*, 15:151–167.

Baumann, S.B., Wozny, D.R., Kelly, S.K., and Meno, F.M. (1997). The electrical conductivity of human cerebrospinal fluid at body temperature. IEEE Trans. Biomed. Eng., 44(3):220–223.

Brindley, G.S. and Lewin, W.S. (1968) The sensations produced by electrical stimulation of the visual cortex. *J. Physiol.,* 196:479–493.

Butovas, S. and Schwarz, C. (2003). Spatiotemporal effects of microstimulation in rat neocortex: a parametric study using multielectrode recordings. *J. Neurophysiol.,* 90(5):3024–39.

Cameron, T. (2004). Safety and efficacy of spinal cord stimulation for the treatment of chronic pain: a 20-year literature review. *J. Neurosurg.*, 100(3 Suppl.):254–267.

Coffey, R.J. (2001) Deep brain stimulation for chronic pain: results of two multicenter trials and a structured review. *Pain Med.*, 2:183–192.

Crile, G.W., Hosmer, H.R., and Rowland, A.F. (1922) The electrical conductivity of animal tissues under normal and pathological conditions. *Am. J. Physiol.*, 60:59–106.

Eisenberg, R.S., and Mathias, R.T. (1980). Structural analysis of electrical properties of cells and tissues. *CRC Crit. Rev. Biomed. Eng.*, 4:203–232.

Grill, W.M. and McIntyre, C.C. (2001). Extracellular excitation of central neurons: implications for the mechanisms of deep brain stimulation. *Thalamus & Related Systems*, 1:269–277.

Grill, W.M. and Mortimer, J.T. (1994). Electrical properties of implant encapsulation tissue. *Ann. Biomed. Eng.*, 22:23–33.

Grill, W.M. and Mortimer, J.T. (1995). Stimulus waveforms for selective neural stimulation. *IEEE Eng. Med. Biol.*, 14:375–385.

Grill, W.M. (1999). Modeling the effects of electric fields on nerve fibers: influence of tissue electrical properties. *IEEE Trans. Biomed. Eng.*, 46:918–928.

Gross, R.E. and Lozano, A.M. (2000). Advances in neurostimulation for movement disorders. *Neurol. Res.*, 22, 247–258.

Gross, R.E. (2004). Deep brain stimulation in the treatment of neurological and psychiatric disease. Expert Rev. Neurother., 4, 465–78.

Gustafsson, B. and Jankowska, E. (1976). Direct and indirect activation of nerve cells by electrical pulses applied extracellularly. *J. Physiol.,* 258:33–61.

Hodaie, M., Wennberg, R.A., Dostrovsky, J.O., and Lozano, A.M. (2002) Chronic anterior thalamus stimulation for intractable epilepsy. *Epilepsia*, 43, 603–608 (2002).

Holsheimer, J., Struijk, J.J., and Tas, N.R. (1995). Effects of electrode geometry and combination on nerve fibre selectivity in spinal cord stimulation. *Med. Biol. Eng. Comput.,* 33:676–682.

Hutchison, W.D., Chung, A.G., and Goldshmidt, A. (2002). Chronaxie and refractory period of neuronal inhibition by extracellular stimulation in the region of rat STN. Program No. 416.3. Abstract Viewer/Itinerary Planner CD-ROM, Society for Neuroscience, Washington, D.C.

Jankowska, E., Padel, Y., and Tanaka, R. (1975). The mode of activation of pyramidal tract cells by intracortical stimuli. *J. Physiol.,* 249:617–636.

Jankowska, E., and Roberts, W.J. (1972). An electrophysiological demonstration of the axonal projections of single spinal interneurones in the cat. *J. Physiol.*, 222:597–622.

Li, C.-H., Bak, A.F., and Parker, L.O. (1968). Specific resistivity of the cerebral cortex and white matter. Exp. Neurol., 20:544–557.

Li, C.L. and Bak, A. Excitability characteristics of the A- and C-fibers in a peripheral nerve. *Exp. Neurol.,* 50:67–79.

Lilly, J.C., Hughes, J.R., Alvord, E.C., Jr, and Galkin, T.A. (1955) Brief noninjurious electric waveform for stimulation of the brain. S*cience*, 121:468–469.

Lipski, J. (1981). Antidromic activation of neurones as an analytic tool in the study of the central nervous system. *J. Neurosci. Methods*, 4:1–32.

McCreery, D.B., Yuen, T.G., Agnew, W.F., Bullara, L.A. (1997). A characterization of the effects on neuronal excitability due to prolonged microstimulation with chronically implanted microelectrodes. IEEE Trans. Biomed. Eng., 44(10):931–939.

McIntyre, C.C. and Grill, W.M. (1999). Excitation of central nervous system neurons by nonuniform electric fields. Biophys. J., 76:878–888.

McIntyre, C.C. and Grill, W.M. (2000). Selective microstimulation of central nervous system neurons. Ann. Biomed. Eng., 28:219–233.

McIntyre, C.C. and Grill, W.M. (2001). Finite element analysis of the current-density and electric field generated by metal microelectrodes. Ann. Biomed. Eng., 29(3):227–235.

McIntyre, C.C. and Grill, W.M. (2002). Extracellular stimulation of central neurons: influence of stimulus waveform and frequency on neuronal output. J. Neurophysiol., 88:1592–1604.

McIntyre, C.C., Grill, W.M., Sherman, D.L., and Thakor, N,.V. (2004). Cellular effects of deep brain stimulation: model-based analysis of activation and inhibition. *J. Neurophysiol.*, 91:1457–1469.

Miocinovic, S. and Grill, W.M. (2004). Sensitivity of temporal excitation properties to the neuronal element activated by extracellular stimulation. J. Neurosci. Methods, 132:91–99.

Nicholson, P.W. (1965). Specific impedance of cerebral white matter. *Exp. Neurol.*, 13:386–401.

Nicolelis, M.A.L., Dimitrov, D., Carmena, J.M., Crist, R., Lehew, G., Kralik, J.D., and Wise, S.P. (2003). Chronic, multisite, multielecrode recording in macaque monkeys. *Proc. Natl. Acad. Sci., U.S.A.*, 100:11041–1046.

Normann, R.A., Maynard, E.M., Rousche, P.J., and Warren, D.J. (1999). A neural interface for a cortical vision prosthesis. *Vision Res.*, 39(15):2577–2587.

Nowak, L.G. and Bullier, J. (1998a). Axons, but not cell bodies, are activated by electrical stimulation in cortical gray matter. I. Evidence from chronaxie measurements. *Exp. Brain Res.*, 118:477–488.

Nowak, L.G. and Bullier, J. (1998b). Axons, but not cell bodies, are activated by electrical stimulation in cortical gray matter. II. Evidence from selective inactivation of cell bodies and axon initial segments. *Exp. Brain Res.*, 118:489–500.

Otto, S.R., Brackmann, D.E., Hitselberger, W.E., Shannon, R.V., and Kuchta, J. (2002). Multichannel auditory brainstem implant: update on performance in 61 patients. *J. Neurosurg.*, 96:1063–1071.

Ranck, J.B., Jr. (1975). Which elements are excited in electrical stimulation of mammalian central nervous system: a review. *Brain Res.*, 98:417–440.

Ranck, J.B., Jr. (1963) Analysis of specific impedance of rabbit cerebral cortex. *Exp. Neurol.*, 7:153–174.

Ranck, J.B., Jr. and BeMent, S.L. (1965) The specific impedance of the dorsal columns of the cat: an anisotropic medium. *Exp. Neurol.*, 11:451–463. 440.

Robblee, L.S. and Rose, T.L. (1990). Electrochemical guidelines for selection of protocols and electrode materials for neural stimulation. In *Neural Prostheses: Fundamental Studies*, Agnew, W.F. and McCreery, D.B., Eds., Prentice-Hall, Englewood Cliffs, NJ, p. 25–66.

Roberts, W.J. and Smith, D.O. (1973). Analysis of threshold currents during microstimulation of fibers in the spinal cord. *Acta Physiol. Scand.*, 89:384–394.

Sances, A., Jr. and Larson, S.J. (1975). Impedance and current density studies. In *Electroanesthesia: Biomedical and Biophysical Studies*, Sances, A. and Larson, S.J., Eds., Academic Press, New York, 1975, p. 114–24.

Schmidt, E.M., Bak, M.J., Hambrecht, F.T., Kufta, C.V., O'Rourke, D.K., and Vallabhanath, P. (1996). Feasibility of a visual prosthesis for the blind based on intracortical microstimulation of the visual cortex. *Brain*, 119:507–522.

Stoney, S.D., Jr., Thompson, W.D., and Asanuma, H. (1968). Excitation of pyramidal tract cells by intracortical microstimulation: effective extent of stimulating current. *J. Neurophys.*, 31:659 669.

Swadlow, H.A. (1992). (1992). Monitoring the excitability of neocortical efferent neurons to direct activation by extracellular current pulses. *J. Neurophysiol.*, 68:605–619.

Tehovnik, E.J. (1996). (1996). Electrical stimulation of neural tissue to evoke behavioral responses. *J. Neursci. Methods*, 65:1–17.

Tkacs, N.C. and Wurster, R.D. (1991). Strength-duration and activity-dependent excitability properties of frog afferent axons and their intraspinal projections. *J. Neurophysiol.*, 65:468–76.

Troyk, P, Bak, M, Berg, J, Bradley, D, Cogan, S, Erickson, R, Kufta, C, McCreery, D, Schmidt, E, and Towle, V. (2003). A model for intracortical visual prosthesis research. *Artif. Organs,* 27:1005 1015.

Velasco, F., Velasco, M., Jimenez, F., Velasco, A.L., and Marquez, I. (2001). Stimulation of the central median thalamic nucleus for epilepsy. *Stereotact. Funct. Neurosurg.*, 77, 228–232.

West, D.C. and Wolstencroft, J.H. (1983). Strength-duration characteristics of myelinated and non-myelinated bulbospinal axons in the cat spinal cord. *J. Physiol.*, 337:37–50.